

Second harmonic generation in dissipative metamaterials

Ye.S. Mukhametkarimov¹, Zh.A. Kudyshev^{1,2}, A.E. Davletov¹,
I.R. Gabitov^{3,4}, A.I. Maimistov^{5,6}, M.G. Stepanov³

¹*Department of Physics, Al-Farabi Kazakh National University
al-Farabi ave., 71, Almaty, 050038, KAZAKHSTAN*

²*Department of Electrical Engineering, University at Buffalo,
State University of New York, 230 Davis Hall Buffalo, New
York 14260-2500, USA*

³*Department of Mathematics, the University of Arizona,
617 N. Santa Rita, Tucson, AZ 85721-0089, USA*

⁴*L.D. Landau Institute for Theoretical Physics, RAS, 1-A
Akademik Semenova av., Chernogolovka, Moscow Region 142432,
RUSSIA*

⁵*Department of Solid State Physics and Nanosystems,
National research nuclear university MEPhI, Kashirskoe sh. 31,
Moscow 115409, RUSSIA*

⁶*Department of Physics and Technology
of Nanostructures, Moscow Institute for Physics and Technology,
Institutskii lane 9, Dolgoprudny, Moscow region 141700,
RUSSIA*

July 27, 2018

Abstract

Second harmonic generation is considered in lossy negative-index metamaterials. It is shown that energy transfer from fundamental to harmonic takes place in the entire sample for the range of phase mismatch values. Note that in conventional case this range collapses to

the point (ideal phase matching). The dependance of the boundary of this range as function of dissipation values is obtained using computer simulations.

1 Introduction

In recent years metamaterials have attracted a great deal of attention in the scientific community. Research in this field is stimulated by necessity for better understanding of fundamentals of the electrodynamics in such materials and also because of the broad range of potential applications[1]-[7]. One of the most unusual type of metamaterials are those with a negative refractive index (NRI) [1], [2]. The main difference of such materials from conventional dielectrics is their left-hand orientation of the fundamental triplet of vectors \mathbf{k} , \mathbf{E} and \mathbf{H} . A consequence of such left-handed orientation is the opposite directionality of the wave vector \mathbf{k} and the Poynting vector \mathbf{S} in NRI materials (NIRM).

Most of currently fabricated NRIM are utilizing plasmonic resonance in metallic structures embedded to dielectric matrix. The sign of the index of refraction in this case is negative only for a limited frequency domain. Nonlinear multi-wave interaction, when part of interacting waves correspond to negative index frequency domain and another part to positive index domain, is very different from conventional multi-wave interaction. In particular case of second harmonic generation, the propagation directions of fundamental and second harmonics are opposite [11]-[15].

In conventional nonlinear dielectrics, efficient energy transfer from fundamental to second harmonic wave takes place only under perfect phase matching. Intensities of fundamental and second harmonics are respectively monotonically decreasing and increasing through the sample. Instead, in the presence of phase mismatch there is alternating energy transfer between harmonics along the sample [17, 18] and field intensities have an oscillatory distribution along a sample. It was been shown [19], that in NRI materials, monotonic energy transfer takes place even in non-ideal phase matching conditions $|\Delta| \neq 0$. Efficient energy transfer occurs within the interval $|\Delta| \leq \Delta_{cr}$, where Δ_{cr} is a critical mismatch value. If the mismatch value is outside of the critical interval, then field intensities are periodically varying along the sample. These results were obtained under the assumption that metamaterials are lossless. However, real metamaterials are lossy [20, 21] and loss values can be significant. While the presence of losses in conventional materials does not change dependance of spatial fields profiles on phase mismatch values, losses may affect the value of Δ_{cr} in negative index materials. This paper considers the process of the second harmonic generation in the presence of losses. In particular, the impact of loss values for both harmonics on the value of critical mismatch and spatial distribution of field intensities are analyzed.

2 Basic equations

Following [19] we assume a refractive index that is negative at the fundamental frequency ω and is positive at the frequency of the second-harmonic wave 2ω . To satisfy the phase matching condition, both wave-vectors must be oriented in the same direction. Therefore fundamental and the second harmonic waves are propagating in opposite directions. The propagation direction of the fundamental wave is assumed to be oriented along the z axes, while the propagation direction of the second harmonic wave is oriented oppositely.

The set of equations in the slowly varying envelope approximation, describing second harmonic generation in a lossy medium with quadratic χ^2 nonlinearity [18, 19] reads as:

$$\begin{aligned}\frac{\partial E_1}{\partial z} &= -\nu\kappa_1 E_2 E_1^* \exp(-i\Delta z) - \alpha_1 E_1, \\ \frac{\partial E_2}{\partial z} &= \nu\kappa_2 E_1^2 \exp(i\Delta z) + \alpha_2 E_2.\end{aligned}\tag{1}$$

Here $\Delta = 2k'_1 - k'_2$ stands for the phase mismatch, $k_{1,2} = k'_{1,2} + ik''_{1,2}$ are the wave numbers of the fundamental and second harmonic correspondingly, $E_{1,2}$ are complex amplitudes of fundamental and second harmonic waves respectively, $\kappa_j = 2\pi\chi^2(\omega_j)\omega_j^2\mu(\omega_j)/(c^2k'_j)$, $j = 1, 2$ denotes a coupling coefficients for fundamental and second harmonic correspondingly, and $\alpha_j = k''_j$ are the corresponding absorption coefficients. The system of equations (1) can be transformed to autonomous form by the following change of variable $E_2(z) \rightarrow E_2(z) \exp(i\Delta z)$:

$$\begin{aligned}\frac{\partial E_1}{\partial z} &= -\nu\kappa_1 E_2 E_1^* - \alpha_1 E_1, \\ \frac{\partial E_2}{\partial z} &= \nu\kappa_2 E_1^2 - i\Delta E_2 + \alpha_2 E_2.\end{aligned}\tag{2}$$

Let the left end of the sample coincide with the origin $z = 0$ and the right end correspond to the point $z = L$. Then the boundary conditions for the set of equations (1) have the following form:

$$E_1(0) = E_{10} \exp(i\varphi_{10}), \quad E_2(L) = 0.\tag{3}$$

Here e_{10} , φ_{10} are real amplitude and phase of the incoming fundamental wave at the left end of the sample. Using rescaling $E_1 = \sqrt{I_0} \mathcal{E}_1(\zeta)$, $E_2 = \sqrt{I_0\kappa_2/\kappa_1} \mathcal{E}_2(\zeta)$, $\zeta = z\sqrt{\kappa_1\kappa_2 I_0}$, $\tilde{\Delta} = \Delta/\sqrt{\kappa_1\kappa_2 I_0}$,

$\tilde{\alpha}_{1,2} = \alpha_{1,2}/\sqrt{\kappa_1\kappa_2 I_0}$, $I_0 = E_{10}^2$, $l = L\sqrt{\kappa_1\kappa_2 I_0}$ system of equations (2) can be rewritten as follows:

$$\begin{aligned}\frac{\partial \mathcal{E}_1}{\partial \zeta} &= -i\mathcal{E}_2\mathcal{E}_1^* - \tilde{\alpha}_1\mathcal{E}_1, \\ \frac{\partial \mathcal{E}_2}{\partial \zeta} &= i\mathcal{E}_1^2 - i\tilde{\Delta}\mathcal{E}_2 + \tilde{\alpha}_2\mathcal{E}_2, \\ \mathcal{E}_1(0) &= 1, \quad \mathcal{E}_2(l) = 0.\end{aligned}\tag{4}$$

It has been shown in [11, 19] that if $\tilde{\alpha}_{1,2} = 0$, then the total energy flux is not changing along the sample: $|\mathcal{E}_1|^2 - |\mathcal{E}_2|^2 = C$. This constant flux plays the role of the Manley-Rowe relation, which in conventional dielectrics represents conservation of energy ($|\mathcal{E}_1|^2 + |\mathcal{E}_2|^2 = C$). In lossy NRI materials, equations for the field intensities read as

$$\begin{aligned}\frac{\partial |\mathcal{E}_1|^2}{\partial \zeta} &= i(\mathcal{E}_1^2\mathcal{E}_2^* - \mathcal{E}_1^{*2}\mathcal{E}_2) - 2\tilde{\alpha}_1|\mathcal{E}_1|^2, \\ \frac{\partial |\mathcal{E}_2|^2}{\partial \zeta} &= i(\mathcal{E}_1^2\mathcal{E}_2^* - \mathcal{E}_1^{*2}\mathcal{E}_2) + 2\tilde{\alpha}_2|\mathcal{E}_2|^2.\end{aligned}\tag{5}$$

Therefore the total flux is not a constant and changes along the sample in accordance to the following relation:

$$\frac{\partial}{\partial \zeta} (|\mathcal{E}_1|^2 - |\mathcal{E}_2|^2) = -2(\tilde{\alpha}_1|\mathcal{E}_1|^2 + \tilde{\alpha}_2|\mathcal{E}_2|^2).\tag{6}$$

This relation determines how the gradient of the total flux is related to the energy dissipation per unit time in the unit of volume and can be viewed as a differential form of Manley-Rowe relation in the presence of losses.

By representing complex amplitudes \mathcal{E}_1 and \mathcal{E}_2 in terms of amplitudes $e_{1,2}$ and phases $\varphi_{1,2}$ and separation of the real and imaginary parts the following set of equations with corresponding boundary conditions can be obtained:

$$\begin{aligned}\frac{\partial e_1}{\partial \zeta} &= e_1 e_2 \sin(\theta) - \tilde{\alpha}_1 e_1, \\ \frac{\partial e_2}{\partial \zeta} &= e_1^2 \sin(\theta) + \tilde{\alpha}_2 e_2, \\ \frac{\partial \theta}{\partial \zeta} &= \left(\frac{e_1^2}{e_2} + 2e_2\right) \cos(\theta) - \tilde{\Delta} \\ e_1(0) &= \exp(i\varphi_{10}), \quad e_2(l) = 0, \quad \theta(l) = -\frac{\pi}{2}.\end{aligned}\tag{7}$$

here $\theta = \varphi_2 - 2\varphi_1$.

The boundary condition for θ can be found by taking into account fact that ratio e_1^2/e_2 in the last equation of the system (7) is singular at the point $\zeta = l$. Since the phase derivative can not be infinite from the point of view of physics, we conclude that $\cos\theta_0 = 0$ (here $\theta(0) = \theta_0$) and $\theta_0 = \pm\pi/2$. The slope of the function $e_2(\zeta)$ must be negative in the neighborhood of $\zeta = l$, therefore, $\theta_0 = -\pi/2$.

Below, two important cases are considered: ideal phase matching condition $\tilde{\Delta} = 0$ and second harmonic generation in the presence of phase mismatch $\tilde{\Delta} \neq 0$.

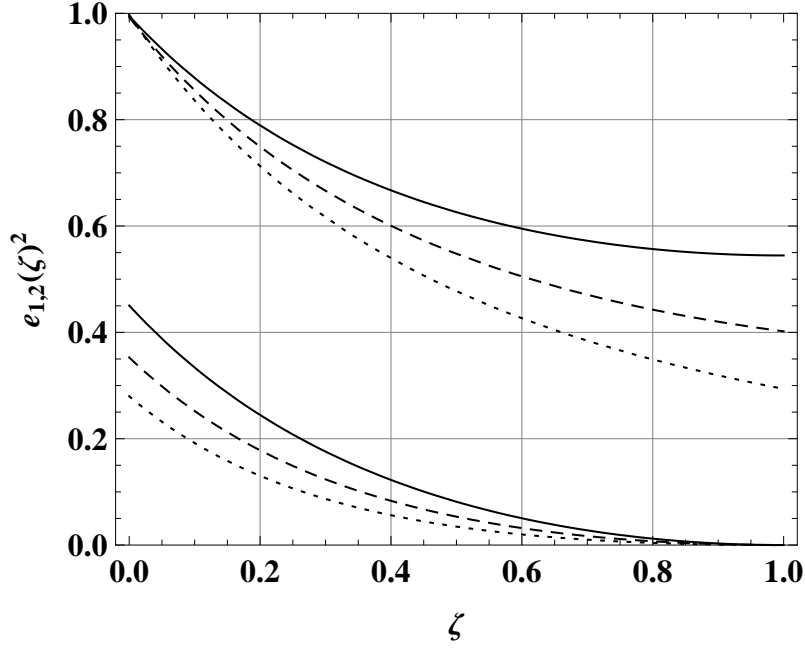
3 Analysis and results of computer modeling

3.1 Ideal phase matching

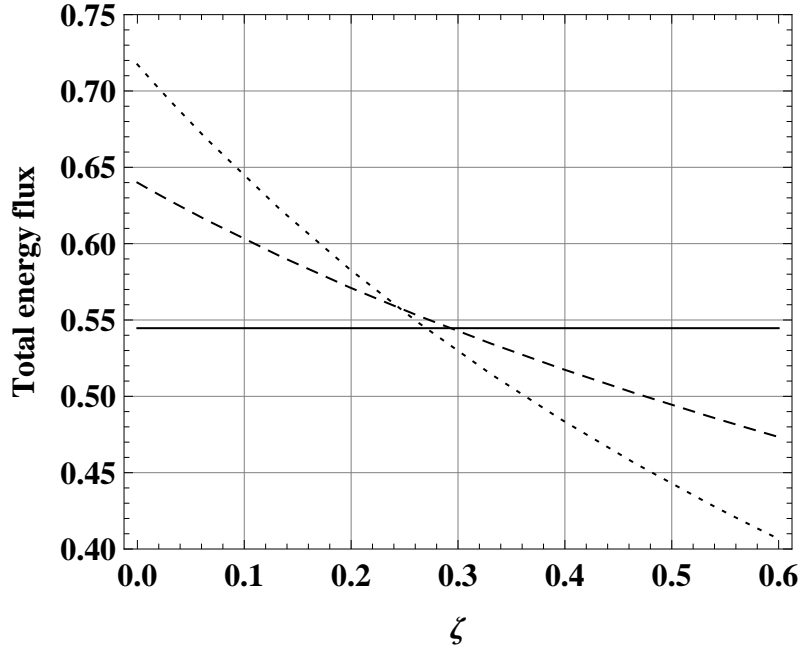
The phase difference $\theta(\zeta)$ is not changing along the sample and $\theta = -\pi/2$ in lossless meta-materials, when $\tilde{\Delta} = 0$ [11, 19]. Therefore second harmonic generation can be described in terms of only two equations for $e_{1,2}$. Presence of losses does not change the equation for θ , therefore $\theta = -\pi/2$ is still a stable stationary solution of the equation for the phase θ in (7). Indeed, since $(e_1^2/e_2 + 2e_2)$ is always positive and $\tilde{\Delta} = 0$, then the right-hand side of the equation for θ has negative slope at the points where $\theta = -(\pi/2)$. Hence, in the case of ideal phase matching, the phase difference is a constant regardless of losses. Losses affect only field intensities. Figure 1 presents results from computer simulations and illustrates spatial distribution of the field intensities at ideal phase matching $\tilde{\Delta} = 0$. Two principal cases are presented on subfigure (a): the medium without and with losses. In the last case values of the dimensionless absorption coefficients are chosen to be $\tilde{\alpha}_1 = 0.2$, $\tilde{\alpha}_2 = 0.1$ and $\tilde{\alpha}_1 = 0.4$, $\tilde{\alpha}_2 = 0.1$.

Figure 1 clearly indicates that the presence of the energy absorption in the medium does not alter the qualitative picture of waves behavior inside the sample, and only contributes an additional decrease in the intensities of the fundamental and the second harmonic waves. It is quite natural that the decrease in the intensities is aggravated by the growth of the corresponding absorption coefficients.

The dependance of a total energy flux $S = e_1^2 - e_2^2$ as function of the coordinate is shown in subfigure (b). Solid line, which corresponds to a lossless case, represents the Manley-Rowe relation. Dotted-dashed and dashed lines in the insert are solutions of the Manley-Rowe relation in differential form (6). Presence of losses leads to the increase of the total flux value at the left end of the sample due to the fact that losses are reducing inverse flux of second harmonic energy. Total flux is monotonically decreasing along the sample since spatial derivative of S is negative (see equation (6)). The impact of losses on conversion efficiency $K = e_2(0)/e_1(0)$ is shown in Figure (2). It was demonstrated in [19], that conversion efficiency in lossless medium with ideal



(a) Profiles intensity of the fields $e_{1,2}(\zeta)^2$ as function of dimensionless coordinate ζ .



(b) Total energy flux of the fields $e_1(\zeta)^2 - e_2(\zeta)^2$ as function of dimensionless coordinate ζ .

Figure 1: The intensity dependence of the fundamental and the second-harmonic waves on the dimensionless coordinate along the sample under the condition of the ideal phase matching - subfigure (a) and spatial distribution of the total energy flux $S = e_1^2 - e_2^2$ - subfigure (b). Solid lines: $\tilde{\alpha}_{1,2} = 0$, dashed lines: $\tilde{\alpha}_1 = 0.2, \tilde{\alpha}_2 = 0.1$, dotted-dashed lines: $\tilde{\alpha}_1 = 0.4, \tilde{\alpha}_2 = 0.1$.

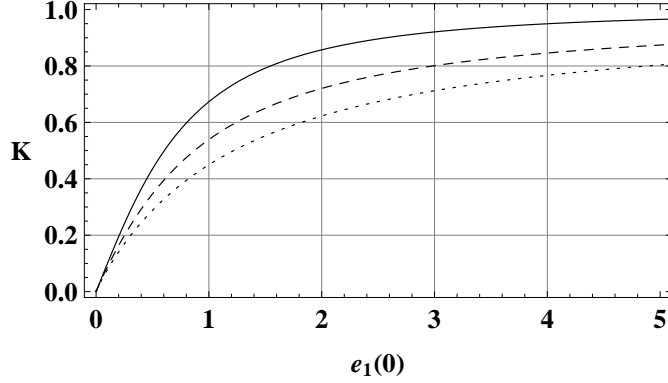


Figure 2: Conversion efficiency $K = e_2(0)/e_1(0)$ as a function of incident pump wave amplitude. Solid, dashed and dotted lines are corresponding to $\tilde{\alpha}_{1,2} = 0$, $\tilde{\alpha}_{1,2} = 0.3$, and $\tilde{\alpha}_{1,2} = 0.6$ respectively.

phase matching asymptotically approaches 1 (total conversion). Losses are slowing growth of conversion efficiency with increase of the amplitude of incident pump wave and reducing its limit value.

3.2 Impact of phase mismatch

3.2.1 Critical phase mismatch in presence of losses.

It has been shown in [19] that in NRI lossless materials monotonic energy transfer from pump to second harmonic field takes place for $|\tilde{\Delta}| \leq \tilde{\Delta}_{cr}$, where $\tilde{\Delta}_{cr}$ is a critical phase mismatch value. Outside of this interval both fields exhibit spatial oscillatory behavior. Since losses are unavoidable in realistic metamaterials, it is of practical interest to analyze an impact of absorption in the medium on the value of critical mismatch $\tilde{\Delta}_{cr}$.

Impact of losses on second harmonic generation is analyzed using computer simulations. Typical spatial profiles of both field intensities for $\tilde{\Delta} = 10$ are shown in Figure 3. Solid lines correspond to the case where $\tilde{\alpha}_{1,2} = 0$, dashed lines stand for $\tilde{\alpha}_1 = 0.2$, $\tilde{\alpha}_2 = 0.1$ and the dotted-dashed lines displayed are for $\tilde{\alpha}_1 = 0.4$, $\tilde{\alpha}_2 = 0.1$. It is clearly seen from Figure 3 that, as in the case of the ideal phase matching, account of losses in the medium does not qualitatively alter the behavior of the wave fields within the sample as a function of the coordinate. This fact strongly suggests that in the presence of dissipation the two above mentioned regimes of the second harmonic generation should remain intact.

Since the change in the character of the field distribution along the sample from the monotonic to the oscillatory regimes occurs gradually, it is appropriate to adopt an explicit criterion for

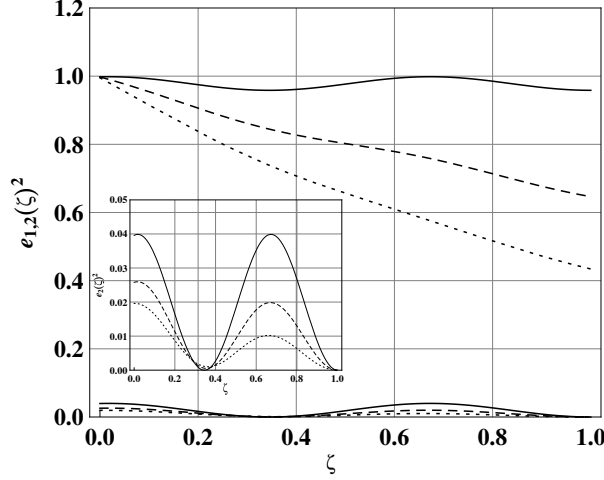


Figure 3: The intensities dependence of the fundamental and the second harmonic waves on the dimensionless coordinate at different values of the absorption coefficients $\tilde{\alpha}_1$ and $\tilde{\alpha}_2$. The phase mismatch is fixed to $\tilde{\Delta} = 10$. Solid lines: $\tilde{\alpha}_{1,2} = 0$, dashed lines: $\tilde{\alpha}_1 = 0.2$, $\tilde{\alpha}_2 = 0.1$, dotted-dashed lines: $\tilde{\alpha}_1 = 0.4$, $\tilde{\alpha}_2 = 0.1$. The insert is an illustration of zoomed in behaviour of the second harmonic field $e_2(\zeta)$.

identifying the critical value of the phase mismatch. It is obvious that a direct application of that criterion for $\tilde{\alpha}_{1,2} = 0$ should reproduce the known theoretical value of the critical mismatch $|\tilde{\Delta}_{cr}| = 4m_1$, here $m_1 \equiv e_1(l)$ (see [19]). This criterion can be introduced using the system of equations (5). The first term in the right hand side of (5) corresponds to the energy exchange between fields. If this term is negative along the sample then energy flows from pump to the second harmonic field. Positive sign of this term corresponds to the inverse process when energy flows from the second harmonic to the pump field. Therefore, the function

$$Q_{\tilde{\Delta},l}(\zeta) = \mathcal{E}_1^2 \mathcal{E}_2^* - \mathcal{E}_1^{*2} \mathcal{E}_2 = \frac{d|\mathcal{E}_1|^2}{d\zeta} + 2\tilde{\alpha}_1 |\mathcal{E}_1|^2 = \frac{d|\mathcal{E}_2|^2}{d\zeta} - 2\tilde{\alpha}_2 |\mathcal{E}_2|^2, \quad (8)$$

can be used for searching $\tilde{\Delta}_{cr}$. Note that energy exchange between harmonics can also be characterized in terms of the angle θ in equations (7). The simplest case when $\tilde{\Delta} = \tilde{\Delta}_{cr}$ corresponds to the situation when energy “flows” from fundamental to second harmonic in all points inside the sample except at ζ_* and $\zeta = l$: $Q_{\tilde{\Delta}_{cr},l}(\zeta) \leq 0$ for $0 \leq \zeta \leq l$ and $Q_{\tilde{\Delta}_{cr},l}(\zeta_*) = 0$, $Q_{\tilde{\Delta}_{cr},l}(l) = 0$ (see equation (5)). The condition $Q_{\tilde{\Delta}_{cr},l}(l) = 0$ is always valid since $\mathcal{E}_2(l) = 0$. Therefore, the critical value of the phase mismatch can be found by solving:

$$Q_{\tilde{\Delta}_{cr},l}(\zeta_*) = 0, \quad (9)$$

with the constrain:

$$Q_{\tilde{\Delta}_{cr},l}(\zeta) \leq 0. \quad (10)$$

Figure 4 represents phase mismatch $\tilde{\Delta}$ satisfying equation (9) as a function of $\tilde{\alpha}_1$. Equation (9) was solved using Newton's method. Both fields $\mathcal{E}_{1,2}(\zeta)$ were found by solving the system of equations (4) assuming that $\tilde{\alpha}_2 = 0$. The sign of the refractive index corresponding to the frequency of fundamental harmonic is negative. In most cases a negative sign of refractive index is achieved using plasmonic resonance in the metallic structures, which leads to considerable losses. Therefore it is reasonable to assume that losses at the second-harmonic frequency are much smaller than the losses on the frequency of the fundamental harmonic.

We considered two cases: when length of the sample is chosen to be $l = 1$ (solid line) and $l = 2$ (dashed line). The amplitude of the incident pump wave in both cases is chosen to be $\mathcal{E}_1(0) = 1$. Numerical simulations showed that the value of critical mismatch is increasing with α_1 . It also follows from computer simulations that $\zeta_* = 0$ for values of $\tilde{\alpha}_1$ in the interval $0 \leq \tilde{\alpha}_1 \leq \bar{\alpha}_1$. In other words, equation (9) in this interval takes the form: $Q_{\tilde{\Delta}_{cr},l}(0) = 0$. Branches on Figure 4 correspond to the multi-valued solutions of the implicit equation $Q_{\tilde{\Delta},l}(0) = 0$ for different values of α_1 .

Part of the lowest branches (solid bold line $l = 1$ or solid dashed line $l = 2$) corresponds to the dependance of the critical value $\tilde{\Delta}_{cr}$ on $\tilde{\alpha}_1$. In this case $Q_{\tilde{\Delta},l}(\zeta) < 0$ for $0 < \zeta < l$. An example of such function $Q_{\tilde{\Delta},l}(\zeta)$ for parameters $\tilde{\alpha}_1 = 0.2$, $l = 1$ is shown in Figure (5), insert (a).

Without loss of generality, we consider the case when $l = 1$. Our analysis shows that the function $Q_{\tilde{\Delta},l}(\zeta)$ is zero at $\zeta = 0$ together with its first derivative $\left(Q_{\tilde{\Delta},l}(0)\right)'_{\zeta} = 0$ when $\tilde{\alpha}_1 = \bar{\alpha}_1$; here $\bar{\alpha}_1 \simeq 0.553$. The profile of the function $Q_{\tilde{\Delta},l}(\zeta)$ in this case is shown in Figure (5), solid line in insert (b).

The remaining part of the lowest branch corresponds to the case when $Q_{\tilde{\Delta},l}(\zeta)$ has one zero inside the interval $0 < \zeta < l$. The profile of such function is shown in Fig. (5), dashed line in the insert (b). This function corresponds to a $\tilde{\Delta}$ which is obtained from equation the equation $Q_{\tilde{\Delta},l}(0) = 0$ for $\tilde{\alpha}_1 > \bar{\alpha}_1$. Note that in this case, the constrain $Q_{\tilde{\Delta}_{cr},l}(\zeta) \leq 0$ is not valid, therefore the corresponding $\tilde{\Delta}$ does not belong to the family of critical values. The values of $\tilde{\Delta}$ on the upper branch correspond to functions of $Q_{\tilde{\Delta},l}(\zeta)$ with several zeros and also do not belong to the family of critical values of phase mismatch.

The dotted line in Figure (4) shows dependance of critical mismatch on $\tilde{\alpha}_1$ for $\tilde{\alpha}_1 \geq \bar{\alpha}_1$ ($l = 1$). The function $Q_{\tilde{\Delta},l}(\zeta)$ corresponding to this case is negative and has one zero within the interval $0 \leq \zeta \leq l$ at $\zeta = \zeta_*$. The derivative of this function with respect to ζ at zero point is also equal

to zero:

$$Q_{\tilde{\Delta},l}(\zeta_*) = 0, \quad \frac{dQ_{\tilde{\Delta},l}(\zeta_*)}{d\zeta} = 0 \quad (11)$$

An example of such function is shown in Figure (5), insert (c). The bold dotted curve is tangential to the lowest branch at the point $\tilde{\alpha}_1 \simeq \bar{\alpha}_1$. Finally, the critical value of mismatch as a function of $\tilde{\alpha}_1$ is shown as a bold curve for $\tilde{\alpha}_1 \leq \bar{\alpha}_1$ and as a bold dotted curve for $\tilde{\alpha}_1 > \bar{\alpha}_1$ ($l = 1$).

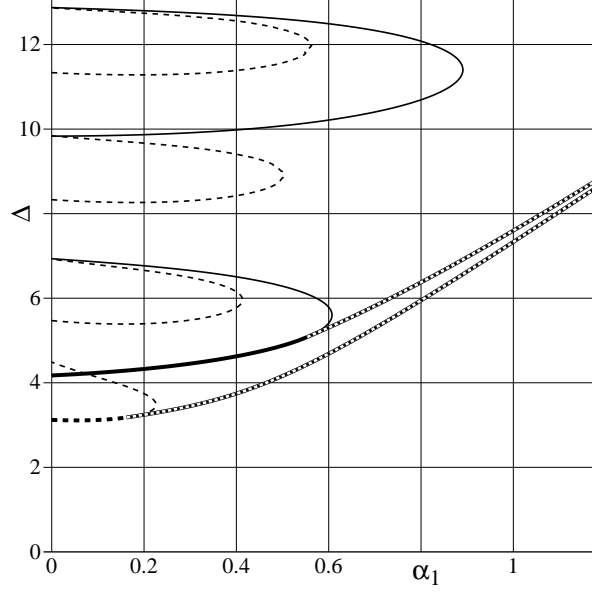


Figure 4: The dependance of $\tilde{\Delta}_{cr}$ as function of of the absorption coefficients $\tilde{\alpha}_1$ ($\tilde{\alpha}_2 = 0$) for the given value of the incoming amplitude of the fundamental wave at the left end of the sample $\mathcal{E}_1(0) = 1$. Solid and dashed tongue-shaped curves lines are corresponding to the solutions of equation $Q_{\tilde{\Delta},l}(0) = 0$ (without constrain $Q_{\tilde{\Delta},l}(\zeta) \leq 0$) for $l = 1$ and $l = 2$ respectively. Part of the lowest branch of the lower curve in each case represents critical value of the phase mismatch $\tilde{\Delta}_{cr} = \tilde{\Delta}_{cr}(\tilde{\alpha}_1)$. In case of $l = 1$ this part (bold solid line) corresponds to the interval $0 \leq \tilde{\alpha}_1 \leq \bar{\alpha}_1$, here $\bar{\alpha}_1 \simeq 0.553$. All values of the function $Q_{\tilde{\Delta},l}(\zeta)$ for $0 \leq \tilde{\alpha}_1 \leq \bar{\alpha}_1$ are satisfying to the constrain (10). Remaining part of this curve and all upper branches are irrelevant since $Q_{\tilde{\Delta},l}(\zeta)$ changes sign inside $0 < \zeta < l$. Dependence of $\tilde{\Delta}_{cr}(\tilde{\alpha}_1)$ at $\tilde{\alpha}_1 \geq \bar{\alpha}_1$ ($l = 1$) is shown by dotted line. This line is tangential to the lower curve of the lowest branch at $\tilde{\alpha}_1 = \bar{\alpha}_1$.

The dependance of the critical mismatch $\tilde{\Delta}_{cr}$ on both absorption coefficients $\tilde{\alpha}_{1,2}$ can be found in a similar way. In case of two variables $\tilde{\alpha}_1$ and $\tilde{\alpha}_2$ each branch (see Fig. 4) will span the corresponding surface. The behavior of $\tilde{\Delta}$, satisfying the equation (9), as function of $\tilde{\alpha}_{1,2}$ is shown

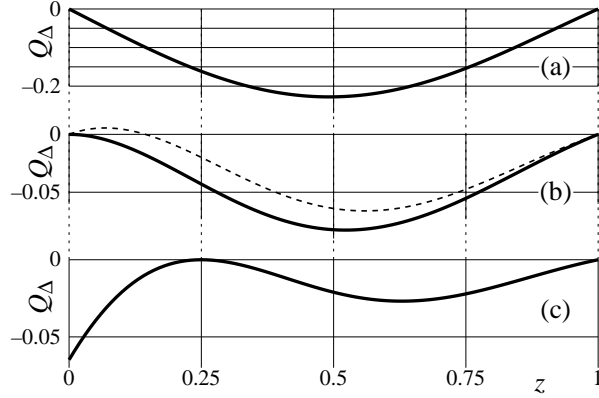


Figure 5: Spatial profiles of the function $Q_{\tilde{\Delta}}(\zeta)$ corresponding to different branches of the solid line on Fig. (4), $l = 1$. a) $\tilde{\alpha}_1 = 0.2$; b) solid line $\tilde{\alpha}_1 \approx 0.553$ and dashed line $\tilde{\alpha}_1 = 0.6$; c) $\tilde{\alpha}_1 \approx 0.814$. In this case, there is maximum at point $\zeta^* = 0.25$, where $Q_{\tilde{\Delta}} = 0$.

on Fig. 6. This figure portrays a two dimensional generalization of the lower part of the lowest branch for $l = 1$ and $\mathcal{E}_1(0) = 1$ shown on Fig. 4. Similarly to the case which is considered above, only part of this surface represents critical values of phase mismatch. The domain of critical values $\tilde{\Delta}_{cr}$ can be found by means of imposing the additional condition $\left(Q_{\tilde{\Delta},l}(0)\right)'_{\zeta} = 0$. Outside of this domain $\tilde{\Delta}_{cr}$ can be found by solving the system of equations (11).

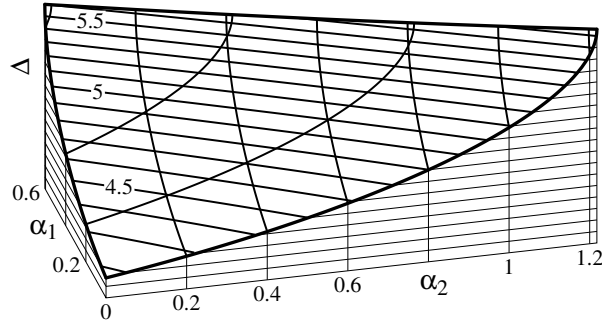
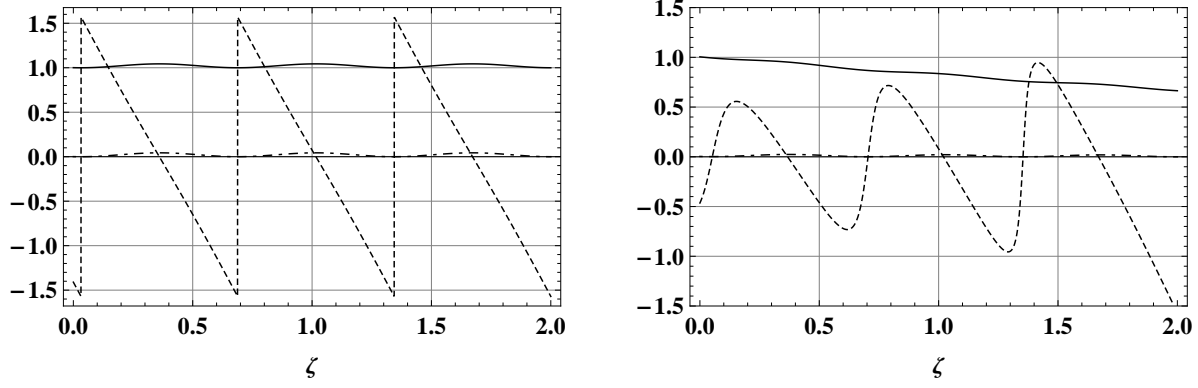


Figure 6: The dependence of the critical phase mismatch $\tilde{\Delta}_{cr}$ on the absorption coefficients $\tilde{\alpha}_1$ and $\tilde{\alpha}_2$ for the given value of the incoming amplitude of the fundamental wave at the left end of the sample $\mathcal{E}_1(0) = 1$.

3.2.2 Field profiles in presence of losses

Second harmonic generation in the subcritical case is similar to the case of ideal phase matching described above. This subsection presents results of computer simulations describing the phase and field profiles along the sample in the supercritical regime. Figure 7 shows an example of spatial profiles corresponding to this regime $\tilde{\Delta} = 10$ for both field intensities $e_{1,2}^2$ and phase θ in the ideal case (Fig.7(a)) and in the presence of losses (Fig. 7(b)). Fig. 7(a) portrays periodic intensity oscillations corresponding to alternating energy exchange between pump and second harmonic fields. Each time the amplitude of second harmonic “touches” zero $e_2 = 0$, the phase θ experiences “ π -phase slip”, similar to a phase slip observed in [23]. Presence of losses leads to a smoothing of this phase jump, which is shown in Fig. 7(b). Note that the value of the phase θ at the end of the sample is $\theta(l) = -\pi/2$ in both cases. Since $\cos(-\pi/2) = 0$, such value of θ eliminates singularity at the right hand side of equation (7) at the end of the sample $\zeta = l$ where $e_2(l) = 0$ and is consistent with negative sign of the derivative $e_2'(\zeta) < 0$ near $\zeta = l$. The intensity profile of the pump field shown in Fig. 7(a) indicates that at the points of maxima, the values of the pump field intensities are greater than intensity of the incident pump field $e_1^2 > e_0^2$. This observation does not contradict conservation of energy. It should be noted that these solutions are representing stationary equilibrium states describing the interaction of two opposite waves. Interaction of these waves in the supercritical regime leads to spatial segmentation of the interval $[0, l]$ to alternating subintervals in which energy flows (in the spectral domain) from fundamental harmonics to second harmonic field and in the next subinterval energy flow changes its direction. Energy flow from fundamental to second harmonics takes place when phase is positive $\theta > 0$. Energy flow in opposite direction takes place when phase is negative $\theta < 0$. As an example let us consider the point $\zeta = l$, where $e_2(l) = 0$. The field $e_2(\zeta)$ is growing while it propagates from right to left, therefore $e_1(\zeta)$ is losing energy and decreasing while it propagates in ζ “direction”. The fact that $e_1(0)$ is less than the maximal value of e_1 inside the sample means that in the neighborhood of the point $\zeta = 0$ energy “flows” from fundamental to second harmonic.

The difference in the behavior of second harmonic intensities without and with losses is illustrated in Fig. 8. In the ideal case (solid line) minimal value of the second harmonic intensity is zero $\min e_2^2 = 0$ and e_2 periodically oscillates along the sample. In the presence of losses $e_2(\zeta)$ is not periodic anymore, $e_2 = 0$ holds only at the end point $\zeta = l$ and minimal values of e_2 are small $e_2(\zeta_{\min}) \ll e_1(\zeta_{\min})$ and increasing from the right to the left. Losses are regularizing sharp π - phase slips, which becomes smooth, wider and smaller than π . Note that a rapid change of $\theta(\zeta)$ takes place in the vicinity of the local minima of $e_2(\zeta_{\min})$. Fig. 7(b) clearly indicates the presence of two scales: a fast scale of the change of $\theta(\zeta)$ near $\zeta \sim \zeta_{\min}$ (positive slope) and a slow change of $\theta(\zeta)$ (negative slope). The slow scale dynamics is determined by the second term $\tilde{\Delta}$ in the right-hand side of the equation for θ of the system (7). The fast dynamics is determined by



(a) Intensity and phase profiles in the ideal case: $\tilde{\alpha}_{1,2} = 0$. (b) Intensity and phase profiles in presence of losses: $\tilde{\alpha}_{1,2} = 0.1$.

Figure 7: Spatial profiles corresponding to supercritical regime $\tilde{\Delta} = 10$ for field intensities $e_{1,2}^2$ and phase θ in the ideal case (left subfigure) $\tilde{\alpha}_{1,2} = 0$ and in presence of losses (right subfigure) $\tilde{\alpha}_{1,2} = 0.1$. Pump intensity, second harmonic intensity and phase θ are labeled as 1, 2 and 3 respectively.

the first term of the right hand side when e_2 becomes small $\varepsilon = e_2(\zeta_{min}) \ll 1$. In the leading order behavior of the “regularized” phase slip the second harmonic field reads as

$$e_2(\zeta) \simeq \sqrt{\varepsilon^2 + e_1^4(\zeta - \zeta_{min})^2} \quad (12)$$

$$\sin \theta(\zeta) \simeq \frac{e_1^2(\zeta - \zeta_{min})}{\sqrt{\varepsilon^2 + e_1^4(\zeta - \zeta_{min})^2}} \quad (13)$$

Comparison of the results obtained by direct computer modeling and from equations (12)-(13) is shown in Fig. 9. Minimum point $\zeta_{min} \approx 0.86875$ and values of $\varepsilon = e_2(\zeta_{min}) \approx 0.01215$, and $e_1(\zeta_{min}) \approx 1$ are taken from the results of computer simulations for $\Delta = 6$, $\alpha_{1,2} = 0.005$ and substituted in equations (12)-(13). Fig. 9 shows that equations (12)-(13) are describing well the “fast” scale supercritical dynamics of the system (7).

4 Conclusion

The process of second harmonic generation in dissipative metamaterials has been studied in case of ideal and non-ideal phase matching. Similarly to lossless medium, the existence of two

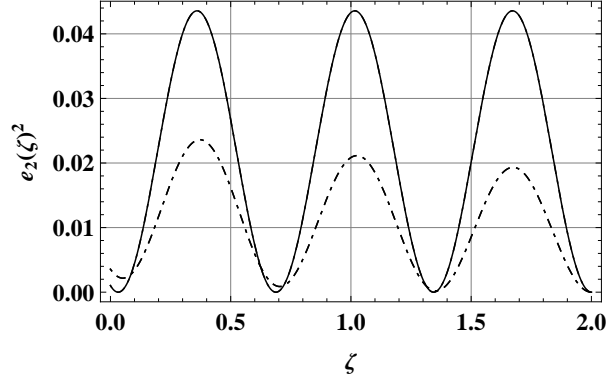
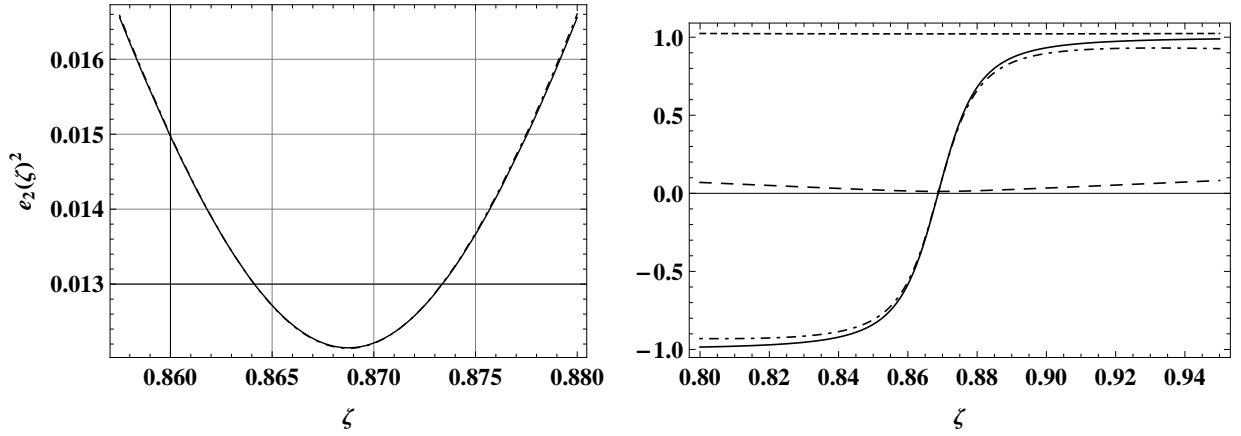


Figure 8: Profiles of intensity second harmonic in presence of losses $\tilde{\alpha}_{1,2} = 0.1$ (dashed line) and lossless case $\tilde{\alpha}_{1,2} = 0$ (solid line) with $\tilde{\Delta} = 10$, $e_1(0) = 1$.



(a) Comparison of the profiles for $e_2(\zeta)$ obtained by computer modeling – dashed line, and by the equation (12) – solid line. As seen from the figure the two curves coincide to the line width.
 (b) Profiles of the fields $e_{1,2}(\zeta)$ and $\sin \theta(\zeta)$ obtained by computer modeling – large-dashed, small-dashed, and dot-dashed lines respectively. Solid line represents $\sin \theta(\zeta)$ given by the equation (13).

Figure 9: Profiles of $e_{1,2}(\zeta)$ and $\sin \theta$ obtained by computer and given by equations (12) - (13), here $\tilde{\Delta} = 6$, $\tilde{\alpha}_{1,2} = 0.005$, $\varepsilon \approx 0.01215$, $\zeta_{min} \approx 0.86875$.

regimes of second harmonic generation was demonstrated theoretically. One regime corresponds to “unidirectional” energy transfer from fundamental to second harmonic and results in monotonic behavior of the field profiles along the sample. Another regime occurs at higher values of the phase mismatch and corresponds to the case when energy flow changes “direction” and leads to oscillatory field profiles along the sample. The critical phase mismatch Δ_{cr} , separating these regimes, depends on the length of the sample and on absorption coefficients of both waves. Analysis of the second harmonic generation in the oscillatory regime shows the difference in behaviour of the electric fields phase difference for the ideal and lossy cases. When phase mismatch value is larger than Δ_{cr} , the phase difference experiences π -phase slip. Presence of losses give a smoothing mechanism of the phase jump and reduces jump’s amplitude

5 Acknowledgments

We would like to thank V. P. Drachev for valuable discussions. AIM, YeM and ZhK appreciate the support and hospitality of the University of Arizona Department of Mathematics during the preparation on this manuscript. This work was partially supported by NSF (Grant No. DMS-0509589), ARO-MURI Award No. 50342-PH-MUR and the State of Arizona (Proposition 301), RFBR (Grants No. 09-02-00701-a and No. 12-02-00561), the Federal Goal-Oriented Program Scientific and Scientific-Educational Personnel of Innovational Russia agreement 8834 and the Ministry Of Sciences and Education of Kazakhstan grant GF3 No/1567.

References

- [1] V.G. Veselago, “The electrodynamics of substances with simultaneously negative values of ε and μ ” Sov. Phys. Usp. 10, 509-514 (1968).
- [2] J.B. Pendry, “Negative Refraction Makes a Perfect Lens”, Physical Review Letters”, **85**(18), 3966 -3969(2000)
- [3] Smith D.R., Schurig D., Pendry J. B., “Some of the waves emitted or reflected”, Appl. Phys. Lett. **81**, 2713-2715 (2002).
- [4] D.J. Robbins, J.B. Pendry, A.J. Holden and W. J. Stewart, “Magnetism from conductors and enhanced nonlinear phenomena”, IEEE Trans. Microwave Theory Tech., **47**(11), 2075 - 2084 (1999)

- [5] D.R. Smith, W.J. Padilla, D.C. Vier, S.C. Nemat-Nasser, and S. Schultz, “Composite Medium with Simultaneously Negative Permeability and Permittivity”, *Phys. Rev. Lett.*, **84**, 4184-4187(2000)
- [6] J.B. Pendry, “Negative refraction makes a perfect lens”, *Phys. Rev. Lett.*, **85**, 39663969 (2000)
- [7] R.A. Shelby, D.R. Smith, and S. Schultz, “Experimental Verification of a negative index of refraction”, *Science* **292**(5514), 77-79(2001), DOI: 10.1126/science.1058847
- [8] A.A. Zharov, I.V. Shadrivov, and Y.S. Kivshar, “Nonlinear properties of left-handed metamaterials”, *Phys. Rev. Lett.*, **91**(037401),1-4(2003).
- [9] M. Lapine, M. Gorkunov, and K.H. Ringhofer, “Nonlinearity of a metamaterial arising from diode insertions into resonant conductive elements”, *Phys. Rev. E*, **67**(065601), 1-4(2003)
- [10] V.M. Agranovich, Y.R. Shen, R.H. Baughman, and A. A. Zakhidov, “Linear and nonlinear wave propagation in negative refraction metamaterials”, *Phys. Rev. B*, **69**(165112), 1-7(2004)
- [11] A.K. Popov and V.M. Shalaev, “Negative-index metamaterials: Second-harmonic generation, Manley-Rowe relations and parametric amplification”, *Appl. Phys. B*, **84**, 131-137(2006)
- [12] M.W. Klein, C. Enkrich, M. Wegener, and S. Linden, “Second-harmonic generation from magnetic metamaterials” *Science*, **313**, 502-504(2006).
- [13] I.V. Shadrivov, A.A. Zharov, and Y.S. Kivshar, “Second-harmonic generation in nonlinear left-handed metamaterials” *J. Opt. Soc. Am. B*, **23**, 529-534(2006).
- [14] D. De Ceglia, A. D’Orazio, M. De Sario, V. Petruzzelli, F. Prudenzano, M. Centini, M. G. Cappendu, M. J. Bloemer, and M. Scalora, “Enhancement and inhibition of second-harmonic generation and absorption in a negative index cavity”, *Opt. Lett.*, **32**, P.265-267(2007).
- [15] M. Scalora, G. D’Aguanno, M. Bloemer, M. Centini, D. de Ceglia, N. Mattiucci, Y.S. Kivshar, “Dynamics of short pulses and phase matched second harmonic generation in negative index materials” *Opt. Express*, **14**, 4746 - 4756 (2006).
- [16] V. Roppo, M. Centini, C. Sibilìa, M. Bertolotti, D. de Ceglia, M. Scalora, N. Akozbek, M. J. Bloemer, J. W. Haus, O. G. Kosareva, V. P. Kandidov, “Role of phase matching in pulsed secondharmonic generation: Walk-off and phase-locked twin pulses in negative-index media, *Phys. Rev. A* **76**, 033829-033840(2007)

- [17] Y.R. Shen, “The principles of non-linear optics”, John Wiley Sons, New York, Chicester, Brisbane, Toronto, Singapore, 1984.
- [18] J.A. Armstrong, N. Bloembergen, J. Ducuing and P.S. Pershan, “Interactions between light waves in a nonlinear dielectric”, *Phys. Rev.* **127**, 1918-1939 (1962).
- [19] Zh. Kudyshev, I.R. Gabitov, A.I. Maimistov, “The effect of phase mismatch on second harmonic generation in negative index materials”, *Phys. Rev. A*, **87**(063840), 1-8 (2013)
- [20] V.M. Shalaev, W. Cai, U. K. Chettiar, H.-K. Yuan, A. K. Sarychev, V. P. Drachev, and A. V. Kildishev, Negative index of refraction in optical metamaterials, *Opt. Lett.*, **30**(24), 3356-3358 (2005)
- [21] S. Xiao, V. Drachev, A. Kildishev, X. Ni, U. Chettiar, H-K.Yuan, and V. Shalaev, “Loss-free and active optical negative index metamaterial”, *Nature*, **466**, 735738 (2010), doi:10.1038/nature09278.
- [22] N.M. Litchinitser, I.R. Gabitov, A.I. Maimistov, and V.M. Shalaev, Negative Refractive Index Metamaterials in Optics, for *Progress in Optics*, edited by E. Wolf, **51**, 1-68 (2008).
- [23] A.I. Chernykh, I.R. Gabitov, E.A. Kuznetsov, Defects of one-dimensional vortex lattices, Singular limits of dispersive waves, Proceedings of a NATO advanced research workshop, Lyons, France, July 8-12, 1991, New York, Plenum, NATO ASI Ser., Ser. B, *Phys.* **320**, 315-328 (1994), ISBN 0-306-44628-6/hbk.